Structural RNA Mimetics: N3′ → P5′ Phosphoramidate DNA Analogs of HIV-1 RRE and TAR RNA Form A-Type Helices That Bind Specifically to Rev and Tat-Related Peptides[†]

C. Ted Rigl,[‡] David H. Lloyd,[§] Dean S. Tsou,[∥] Sergei M. Gryaznov,*[,§] and W. David Wilson*[,‡]

Department of Chemistry, Georgia State University, Atlanta, Georgia 30303, Lynx Therapeutics, Inc., 3832 Bay Center Place, Hayward, California 94545, and Applied Biosystems Division of Perkin-Elmer, Foster City, California

Received August 7, 1996; Revised Manuscript Received October 24, 1996[⊗]

ABSTRACT: An attractive strategy for the development of anti-retroviral drugs is the exploration of compounds that mimic RNA control regions of the viral genome and act as "decoys" to sequester viral gene regulatory proteins. Decoys consisting of RNA, however, are chemically unstable and readily degraded by cellular nucleases. DNA decoys, which are slightly more stable, also might not be appropriate because of possible structural differences between RNA and DNA helices and the complexes they form with proteins. It was recently reported, however, that DNA analogs with modified N3′ → P5′ phosphoramidate sugar−phosphate backbones are stable and nuclease-resistant and exist predominately as A-form helices in solution [Gryaznov, S., et al. (1995) *Proc. Natl. Acad. Sci. U.S.A. 92*, 5798−5802]. We now report that oligonucleotide N3′ → P5′ phosphoramidate DNA analogs of HIV-1 RRE IIB and TAR RNA form stable duplexes that exist in the A form as judged by circular dichroism (CD). Moreover, gel shift assays demonstrate that these phosphoramidates can specifically bind to peptides derived from HIV-1 Rev and Tat proteins. Isosequential phosphodiester DNA duplexes, existing in the B form by CD, do not bind to the respective peptides under the experimental conditions used. These results suggest the possibility that nuclease-resistant oligonucleotide N3′ → P5′ phosphoramidates might serve as RNA-like decoys and disrupt specific viral RNA/protein interactions such as RRE/Rev and TAR/Tat in HIV-1.

Regulation of replication in HIV-1 requires essential binding of two trans-acting proteins, Rev and Tat, to two respective cis-acting RNA binding sites, RRE and TAR (Malim et al., 1989; Rosen et al., 1985). Tat is a transcription activator, while Rev allows partially or unspliced viral RNAs to be transported to the cytoplasm. Rev has been called a "molecular rheostat" for its role as a negative regulator of its own and Tat synthesis and as a positive regulator of the translation of partially spliced RNAs (Cullen & Malim, 1991; Mann et al., 1994). These regulatory proteins provide tight control over HIV-1 replication and efficient use of the limited nucleotide sequences in the viral genome. The key roles of these viral proteins make them attractive targets for drug intervention, but there are as yet no good clinical candidates that target Rev or Tat. A complementary drug strategy is targeting of the structural RNA receptors of these proteins much as DNA has been successfully targeted by anticancer drugs such as the anthracyclines (Weiss et al., 1992) and some minor groove-binding compounds (Mountzouris & Hurley, 1996). Several small cationic molecules that selectively target the RRE RNA have been discovered, and development of such compounds as antiviral drugs is a promising new area of research (Zapp et al., 1993; Ratmeyer et al., 1996).

An alternative strategy for preventing the formation of RRE/Rev and TAR/Tat complexes that has been successfully used to inhibit HIV-1 replication in preliminary studies features endogenous therapeutic RNA or protein decoys produced *in vivo* through genetic manipulation (Bevec et al., 1994; Clusel et al., 1995; Gilboa & Smith, 1994; Lee et al., 1995; Malim et al., 1992). A decoy is designed to mimic the structure of a target molecule that is essential to the progress of a disease. This mimicry enables the decoy to compete with the target molecule as it attempts to interact with specific molecules within the cell. Conversion of this approach to exogenous RNA decoys offers an attractive strategy for antiviral drug development. The RRE control region found in HIV-1 (Figure 1a) is a good possibility for a therapeutic decoy because of the essential role RRE plays in the course of HIV-1 infection (Cullen & Malim, 1991), its specific interaction with Rev protein (Cook et al., 1991; Kjems et al., 1991; Tiley et al., 1992), as well as its highly conserved RNA sequence and structure (Gilboa & Smith, 1994; Symensma et al., 1996).

The most obvious RRE decoy is an RNA molecule with the exact sequence and secondary structure of the region of RRE known to be bound by the Rev protein, the RRE IIB region (Figure 1a) (Malim et al., 1989). This region has been successfully modeled as an RNA hairpin (HP1, Figure 2b) (Tan et al., 1993), as a short RNA hairpin (HP2, Figure 2b) (Bartel et al., 1991), and as an RNA duplex (Figure 2b) (Pritchard et al., 1994). Unfortunately for the designers of exogenous decoys, the stability of RNA in the presence of cellular nucleases is poor, so only *in vivo* expression of an endogenous RNA RRE IIB decoy is plausible. Isosequential DNA decoys could have slightly better stability; however, the helical structure of DNA is B-form, and studies have shown that phosphodiester-linked DNA analogs of RRE

[†] This work was supported by NIH grants to W.D.W.
* Authors to whom correspondence should be addressed.
[‡] Georgia State University.
[§] Lynx Therapeutics, Inc.
[∥] Applied Biosystems Division of Perkin-Elmer.
[⊗] Abstract published in *Advance ACS Abstracts,* January 1, 1997.

S0006-2960(96)01980-0 CCC: $14.00 © 1997 American Chemical Society

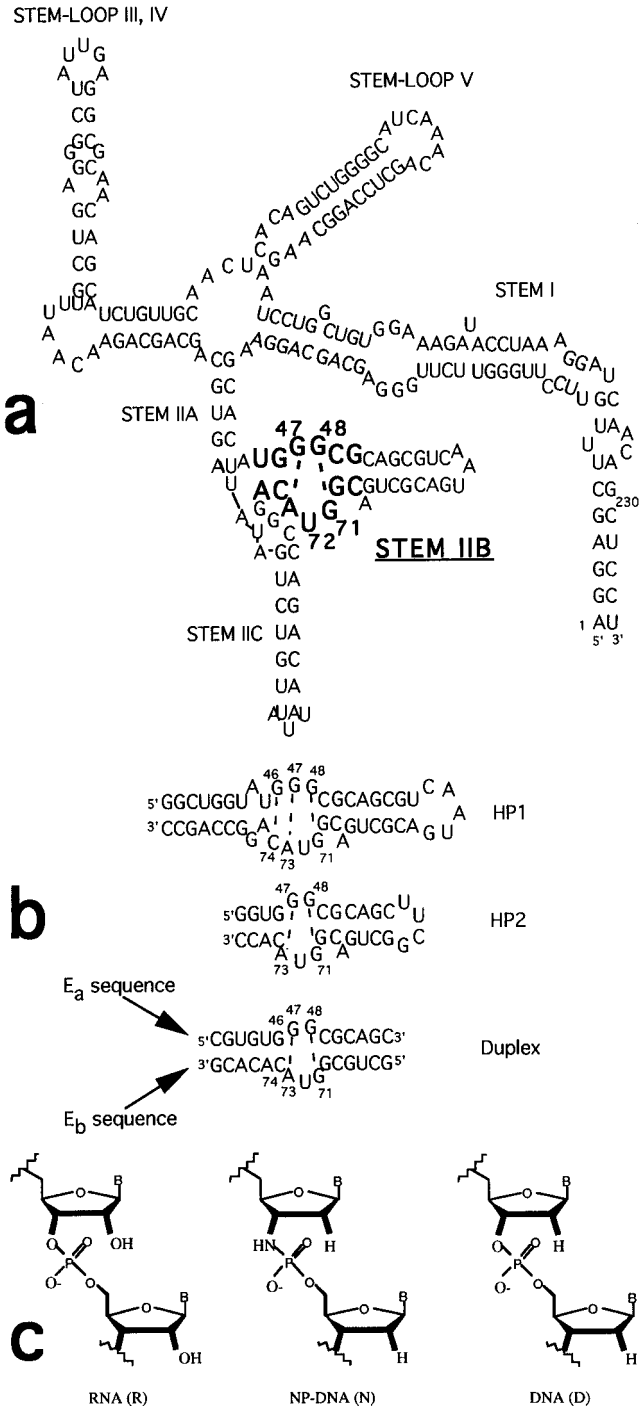

FIGURE 1: (a) Sequence and predicted secondary structure of the Rev-responsive element (RRE) originally defined by Malim et al. (1989) and further characterized by Mann et al. (1994). Stem IIB, which contains the Rev binding element (RBE), is highlighted. Base interactions elucidated by Bartel et al. (1991) using a minimal Rev binding element are represented by dotted lines. (b) Hairpin (HP1 and HP2) and duplex models of the minimal Rev binding element (RBE). Numbering and base interactions are the same in parts a and b. HP1 was defined by Tan et al. (1993), HP2 by Bartel et al. (1991), and the duplex by Pritchard et al. (1994). The notations E_a and E_b are used in this report to define the upper strand and lower strand sequences of the RRE IIB duplex as shown. Duplexes are denoted as E_a/E_b or a/b. (c) Structure of the O3′ → P5′ phosphodiester linkage of RNA, the N3′ → P5′ phosphoramidate linkage of NP-DNA, and the O3′ → P5′ phosphodiester linkage of DNA. The notations R, N, and D are used in this report to define RNA, NP-DNA, and DNA oligonucleotides, respectively. Oligonucleotide RRE linkages in a given homoduplex, for example, might be R-E_a/R-E_b or, in the context of RRE, simply R/R. A given RRE DNA/RNA heteroduplex might be D-Ea/R-Eb or D/N.

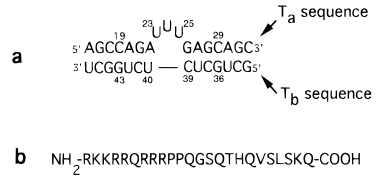

FIGURE 2: (a) Sequence and predicted secondary structure of the minimal binding element of HIV-1 TAR as defined by Pritchard et al. (1994). (b) Sequence of the Tat-24 peptide, which was derived from HIV-1 Tat protein and defined by Long and Crothers (1995). The notations for sequences, T_a and T_b, and oligonucleotides and linkages (R, N, and D) are analogous to the notations used for RRE in parts b and c of Figure 1.

do not bind to Rev (Iwai et al., 1992; Nelson et al., 1996; Pritchard et al., 1994). Deoxyoligonucleotides with modified backbones such as phosphorothioates would have even better stability, but the resulting B-form helical character would prevent their binding to Rev (Tan et al., 1993). It was recently reported, however, that oligodeoxyribonucleotide N3′ → P5′ phosphoramidates (NP-DNA, Figure 1c) form very stable duplexes, are nuclease-resistant, exist predominately as A-form helices in solution, and carry the same formal charge as RNA (DeDionisio & Gryaznov, 1995; Ding et al., 1996; Gryaznov et al., 1995). These observations suggest that NP-DNAs could function as RNA mimetics in an exogenous therapeutic strategy. In spite of their A-form structure, however, these are DNA oligonucleotides, and it was not clear that they could bind significantly to RNA-binding proteins such as Rev and Tat without the involvement of any ribose sugars.

To determine if oligodeoxyribonucleotide N3′ → P5′ phosphoramidates (NP-DNAs) can serve as an RNA mimetic (or decoy) and competitively inhibit RRE IIB and Rev interaction, we selected the duplex model of RRE IIB elucidated by Pritchard et al. (1994) (Figure 1b). This duplex contains bases found to be essential for Rev binding as assessed by *in vitro* selection (Bartel et al., 1991; Kjems et al., 1992). The validity of duplex models is further supported by Wang et al. (1996), who recently demonstrated, using a photo-cross-linking technique, that a similar TAR duplex maintains specific binding contacts with Tat. For our purposes, duplex models, as opposed to hairpin models, facilitate the formation of a variety of homo- and heteroduplexes composed of RNA, NP-DNA, and DNA oligonucleotides, which become variables that can assist in the analysis of complexes formed with Rev and Tat. Appropriate RRE and TAR-related oligonucleotides of RNA, NP-DNA, and DNA were synthesized (Figures 1b,c and 2 and Table 1). The RRE RNA hairpin structures, HP1 and HP2 (Figure 1b), were transcribed *in vitro* (Milligan & Uhlenbeck, 1989) for comparison with the RRE duplexes under study. Limited studies were also conducted with a TAR duplex (Figure 2; Pritchard et al., 1994) to provide a second system for the analysis of the effect of N3′ → P5′ phosphoramidate linkages in RNA/protein interactions.

The RNA-binding sites of Rev and Tat were modeled by truncated peptides. The Rev_{34-50} peptide sequence is in Materials and Methods, and the Tat-24 sequence is in Figure 2. These peptides have a demonstrated ability to maintain the necessary RNA/protein contacts required for high-affinity binding and specificity for RRE IIB and TAR RNAs, respectively (Kjems et al., 1992; Long & Crothers, 1995; Tan et al., 1993). The Rev_{34-50} peptide is one of a series of

Table 1: RRE and TAR Oligonucleotides[a]

oligonucleotide	backbone	sequence	self-stacking[b]
R-E_a	R	E_a	yes
R-E_b	R	E_b	yes
N-E_a	N	E_a	yes
N-E_b	N	E_b	yes
D-E_a	D	E_a	no
D-E_b	D	E_b	no
R-T_a	R	T_a	yes
R-T_b	R	T_b	yes
N-T_a	N	T_a	yes
N-T_b	N	T_b	yes
D-T_a	D	T_a	no
D-T_b	D	T_b	no

[a] Oligonucleotides in this report are denoted by backbone and sequence (see Figures 1b,c and 2). For example, an RNA oligonucleotide with an RRE duplex sequence E_a is denoted R-E_a. [b] Thermal dissociation experiments, along with denaturing and nondenaturing gel electrophoresis, were used to identify apparent self-stacking and similar secondary structures.

related Rev_{34-50} peptides (A−D) that were synthesized as probes of the fidelity of the RRE/Rev interaction (Tan et al., 1993). The duplex models of RRE IIB and TAR and the peptides Rev_{34-50} (A−D) and Tat-24 provide simple minimal representations of RRE IIB/Rev and TAR/Tat interactions and were used to determine the extent to which N3′ → P5′ phosphoramidate DNAs can mimic RNA secondary structures.

Duplexes were studied by UV and circular dichroism spectroscopy to determine the stability and conformation of the helical structures involved. Relative binding affinities for peptides were determined by gel shift analysis. Competitive format gel shift assays were also performed where ^{32}P-labeled RNA duplexes (Figure 1b or 2) were allowed to form complexes with Rev or Tat peptides in the presence of increasing concentrations of unlabeled duplex competitors. The results presented below demonstrate that NP-DNAs can interact strongly and specifically with Rev and Tat. Exogenous decoy strategies utilizing N3′ → P5′ phosphoramidate linkages add a new dimension to the search for antiviral therapies.

MATERIALS AND METHODS

Oligonucleotides. Oligoribonucleotides (termed RNA or R) were prepared on an ABI 380B synthesizer using standard RNA assembly protocols *via* the phosphoramidite method. Oligodeoxyribonucleotide N3′ → P5′ phosphoramidates (termed NP-DNA or N) CGUGUGGGCGCAGC and GCUGCGGUACACACG, the RRE duplex (Figure 1b), and AGCCAGAUUUGAGCAGC and GCUGCUCUCUGGCU, the TAR duplex (Figure 2), were synthesized as described in Chen et al. (1995). Phosphodiester-linked oligodeoxyribonucleotides (termed DNA or D) were synthesized on an ABI 380B synthesizer using a standard assembly protocol *via* the phosphoramidate method. All NP-DNA and DNA sequences used in peptide binding studies contained d(U) bases instead of d(T) bases.

All oligonucleotides used for the duplex model were end-labeled using [γ-^{32}P]ATP and T4 polynucleotide kinase under standard conditions (Amersham). Oligodeoxyribonucleotide primer and templates for the *in vitro* transcription of RRE IIB hairpins, HP1 and HP2 (Figure 1b), were synthesized as described above for DNA using the sequence recommendations provided in a commercially available *in vitro* transcription kit (Ambion; Milligan & Uhlenbeck, 1989). HP1 and HP2 hairpins were transcribed using T7 RNA polymerase in the presence of added [α-^{32}P]UTP (U.S. Biochemical). Reactions were quenched after 2 h, and the transcripts were purified using 12% denaturing polyacrylamide gel electrophoresis. RNA was precipitated, washed with ethanol, and then dried *in vacuo*.

Peptides. Four Rev_{34-50} peptide analogs (A−D) with the sequence defined by Tan et al. (1993) and one Tat-24 peptide with the sequence defined by Long et al. (1995) (Figure 2) were synthesized. The Rev_{34-50} peptide sequence is TRQARR^{39}NRRRRWRERQR, and the analogs are as follows: (A) su-Rev(R^{39})-am, (B) su-Rev(R^{39}→K)-am, (C) NH_2-Rev(R^{39})-COOH, and (D) NH_2-Rev(R^{39}→K)-COOH. Peptides A and B are succinylated (su) at amino termini and amidated (am) at carboxy termini. Peptides were analyzed by HPLC, mass spectrometry (Rev_{34-50} peptides A−D and Tat-24), peptide sequencing (Rev_{34-50} peptides C and D and Tat-24), and gel electrophoresis.

Thermal Dissociation Experiments. Thermal dissociation studies were performed with a Cary 3 spectrophotometer interfaced to a Dell/486 computer as previously described (Kibler-Herzog et al., 1990) at a duplex concentration of 1−3 μM in 10 mM phosphate, 1 mM EDTA, 0.1 M NaCl, and 1 mM $MgCl_2$ at pH 7.0. T_m values were determined from first-derivative plots (Wilson et al., 1996).

CD Spectroscopy. CD spectra were obtained using a JASCO J-710 spectropolarimeter with oligonucleotide duplexes at 1 μM in 10 mM phosphate, 1 mM EDTA, 0.1 M NaCl, and 1 mM $MgCl_2$ at pH 7.0. Rev peptides were diluted to 6 μM on the basis of absorbance at 278 nm (ϵ = 5600 M^{-1} cm^{-1}; Creighton, 1993) in the same buffer. Solutions were scanned from 320 to 190 nm at 5 °C in a 1 cm path length cuvette. Ten scans per solution were averaged, converted to molar ellipticity, [ϵ], and plotted against wavelength.

Gel Shift Assays for RRE/Rev and TAR/Tat Complexes. ^{32}P-internally labeled, self-complementary strands (hairpin models) or mixtures of ^{32}P-5′-end-labeled, complementary strands for duplex models (Figures 1b and 2) were heated to 90 °C for 2 min and then cooled to room temperature to form RRE IIB and TAR models at 1 μM in 10 mM phosphate, 1 mM EDTA, and 0.1 M NaCl at pH 7.0. RRE or TAR models were then diluted and added to a binding reaction buffer. The model-containing solutions were aliquoted (8 μL), and increasing levels of Rev_{34-50} or Tat-24 peptides were added (2 μL) to achieve final peptide concentrations ranging from 0 to 1.4×10^{-4} M. The final reaction conditions in a 10 μL total volume were 10 mM phosphate, 1 mM EDTA, 0.1 M NaCl, 1 mM $MgCl_2$, 1 mM DTT, 170 μg/mL yeast tRNA (Sigma), and 10% glycerol. The reaction mixtures were incubated for 15 min in an ice bath, and samples (3 μL) were then applied to a 12% nondenaturing polyacrylamide gel (20 × 20 cm) cast in 1X TBE (90 mM TRIS/borate and 2 mM EDTA at pH 7.7) that had been equilibrated for 2 h (Sambrook et al., 1989). The samples were electrophoresed for 4 h at 220 V at 6 °C. The gels were fixed, dried *in vacuo* at 80 °C, and autoradiographed (Biomax, Kodak). Autoradiographs were scanned and quantitated (PDI, Inc.).

Competitive Gel Shift Assays for Inhibitors of RRE/Rev and TAR/Tat Complexation. RRE IIB or TAR RNA ^{32}P-labeled duplexes were formed as described above and added to binding reaction buffer (5−25 nM, final). The solutions were aliquoted (8 μL) into reaction vials. Duplex decoys (unlabeled) were formed as described above, diluted with buffer, and then added (2 μL) to the reaction vials. Labeled RNA duplex and duplex decoys were premixed in reaction buffer to prevent premature interaction with Rev or Tat peptides as described by Daly et al. (1993). Rev_{34-50} peptide A or Tat-24 peptide was then added (2 μL) to achieve final desired peptide concentrations. Incubation, electrophoresis, and imaging were the same as described above.

RESULTS

Oligonucleotide Labeling and Characterization

The relative degree of 5′-end-labeling with [γ-^{32}P]ATP of RRE and TAR oligonucleotides made of RNA, NP-DNA, or DNA (Figures 1b and 2; Table 1) was assessed by denaturing polyacrylamide gel electrophoresis and microdensitometry. All RNA and DNA phosphodiester-linked oligonucleotides were efficiently end-labeled; however, the RRE N-E_b and TAR N-T_a and N-T_b oligonucleotides were end-labeled at less than 5%. Only the RRE N-E_a oligonucleotide could be end-labeled at levels comparable to that of isosequential RNA and DNA.

Labeled RRE and TAR oligonucleotides, homoduplexes, and heteroduplexes exhibited the expected relative mobilities under denaturing and nondenaturing PAGE conditions. RNA oligonucleotides and hairpins showed broad bands under nondenaturing PAGE conditions. To visualize all oligonucleotides regardless of end-labeling efficiency, all RRE and TAR oligonucleotides were analyzed by electrophoresis under denaturing conditions and developed with Stainsall (Biorad). A single band of expected relative mobility was detected in each lane. All RRE and TAR RNA oligonucleotides (including hairpins) showed additional minor bands of lower mobility, which were not characterized further. No minor bands were noted for any of the NP-DNA or DNA strands. These observations provided further evidence that all oligonucleotides were pure and that three NP-DNA oligonucleotides, N-E_b, N-T_a, and N-T_b, are end-labeled inefficiently.

Thermal Dissociation Experiments

Results for the RRE system are shown in Table 2. The RNA homoduplex, E1, dissociates at a higher temperature than the isosequential DNA homoduplex, E3. The RRE NP-DNA homoduplex, E2, has an elevated T_m value, consistent with studies of NP-DNA homoduplexes (Ding et al., 1996; Gryaznov et al., 1995). Also consistent with previous studies is the observation that the RNA/NP-DNA heteroduplexes (E4 and E6) dissociate at higher temperatures than the corresponding RNA/DNA heteroduplexes (E5 and E8, respectively). These results extend previous observations of the exceptional stability of NP-DNA-containing duplexes to include duplexes with unusual structural features such as those found in the structural loops and bulges of the RRE sequence.

Thermal dissociation experiments of RRE single-stranded oligonucleotides showed additional evidence of secondary structure, as summarized in Table 1. Noncooperative hyperchromic shifts were particularly evident for the RNA oligonucleotide, R-E_a, and the NP-DNA oligonucleotides, N-E_a and N-E_b. These results are consistent with strand behavior observed during nondenaturing gel electrophoresis. Pronounced base self-stacking at the 5′ end might be responsible for the poor end labeling of the NP-DNA oligonucleotide, N-E_b.

The broad, noncooperative hyperchromic shifts noted for the thermal dissociation of RRE duplexes, E2 (R/R) and E4 (R/N), were inconsistent with our previous reports on fully complementary NP-DNA oligonucleotides (Ding et al., 1996; Gryaznov et al., 1995). To confirm that all oligonucleotide strands can form duplexes with base pair mismatches as in RRE, we combined each oligonucleotide with a fully complementary oligodeoxyribonucleotide (fcDNA) strand, as shown in Figure 3. Results from thermal dissociation experiments of duplexes C1−C6 are presented in Table 3. Sharp, cooperative dissociation curves were observed in every case. The N-E_b oligonucleotide in duplex C4, however, did demonstrate hyperchromicity in the low-temperature end (50−60 °C) of the dissociation process. The

Table 2: RRE Models[a] and T_m Values

models	name	E_a	E_b	T_m (°C)
hairpins	HP1	−	−	ND[b]
	HP2	−	−	62.0
homoduplexes	E1	R	R	54.2
	E2	N	N	58 (broad)
	E3	D	D	44.2
heteroduplexes	E4	R	N	54 (broad)[c]
	E5	R	D	45.0
	E6	N	R	60.8
	E7	N	D	52.2
	E8	D	R	41.5
	E9	D	N	51 (broad)

[a] Model duplexes in this report are denoted by name where E1 is an RRE homoduplex with oligomers R-Ea/R-Eb or, in the context of RRE, simply R/R. [b] ND means not determined. [c] Broad refers to the shape of the first-derivative plot of absorbance versus temperature and suggests a noncooperative thermal denaturation process.

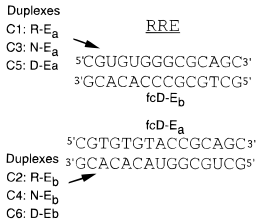

FIGURE 3: RRE RNA, NP-DNA, and DNA oligonucleotides as fully complemented duplexes with DNA (fcDNA). Thermal dissociation results for these duplexes are shown in Table 3.

Table 3: T_m Values for RRE RNA, NP-DNA, and DNA Oligonucleotides as Fully Complemented Duplexes with DNA[a]

models	duplex	Ea	Eb	T_m (°C)
RRE RNA	C1	R	fcD	63.7
	C2	fcD	R	59.1
RRE NP-DNA	C3	N	fcD	72.6
	C4	fcD	N	68.3
RRE DNA	C5	D	fcD	61.5
	C6	fcD	D	60.2

[a] Fully complementary DNAs are denoted fcD-E_a or -E_b, which are complementary to RRE duplex sequences shown in Figure 1b. The resulting fully complemented duplexes are shown in Figure 3.

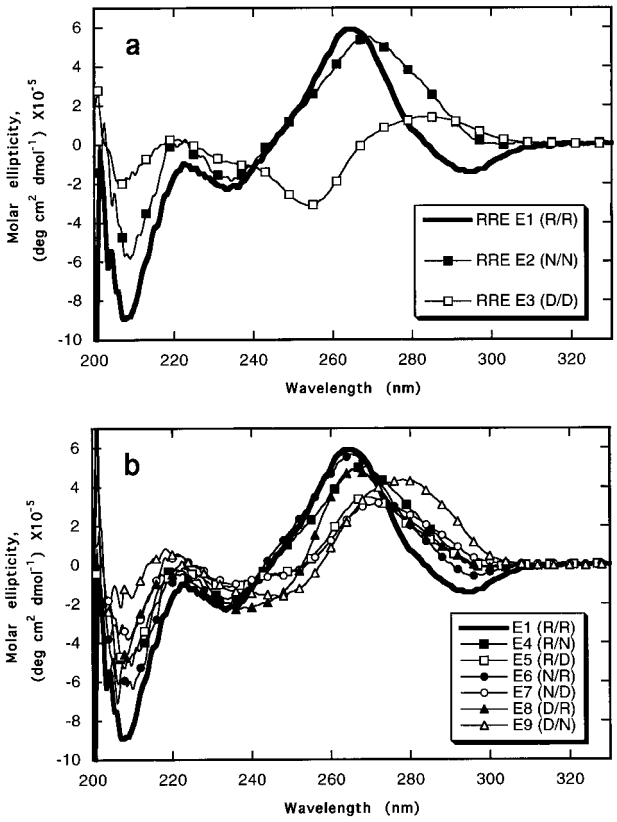

FIGURE 4: (a) CD spectra of the RRE homoduplexes: E1 (R/R), E2 (N/N), and E3 (D/D). (b) CD spectra of the RRE homoduplex, E1 (R/R), shown as a reference and the RRE heteroduplexes: E4 (R/N), E5 (R/D), E6 (N/R), E7 (N/D), E8 (D/R), and E9 (D/N). Note how the filled and unfilled symbols loosely segregate the duplexes into A form (filled) and B form (unfilled) helical families.

T_m values of the RRE NP-DNA/fcDNA heteroduplexes (C3 and C4) were markedly elevated relative to those of the RNA/fcDNA duplexes (C1 and C2), which in turn had greater T_m values than the DNA/fcDNA duplexes (C5 and C6). These results are consistent with our previous reports on fully complementary NP-DNA duplexes (Ding et al., 1996; Gryaznov et al., 1995).

CD Spectroscopy

CD spectroscopy provides very useful information for classification of duplexes in the general A-form or B-form helical family. The RRE homoduplex (E1) has a classical A-form curve shape, while the DNA homoduplex (E3) has a B-form curve shape (Figure 4a). Consistent with previous reports (Ding et al., 1996; Gryaznov et al., 1995), the RRE NP-DNA homoduplex E2 clearly falls into the A-form helical family, but there are observable differences from the RNA homoduplex (E1) in the smaller negative bands at 210 and 290 nm. The positive band is shifted from 265 nm in the RNA homoduplex (E1) to a longer wavelength, 268 nm, in the NP-DNA homoduplex (E2).

CD spectra of RRE heteroduplexes are presented in Figure 4b, and they fall into two general groups. The RNA/NP-DNA heteroduplex, E6 (N/R), has an A-form spectrum particularly at the 210 and 290 nm negative and 265 nm positive bands. The E6 spectrum is nearly superimposable in the 220−270 nm region with the RNA E1 spectrum. Interestingly, the spectrum of the converse RNA/NP-DNA heteroduplex, E4 (R/N), is most similar to the spectrum of the NP-DNA homoduplex, E2 (N/N), at the 210 and 290 nm negative and 268 nm positive bands, as well as in the 220−270 nm region.

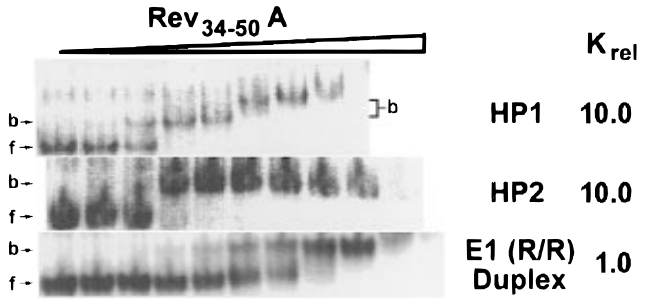

FIGURE 5: Gel shift assays of RRE IIB models HP1, HP2, and RNA duplex (E1, R/R) titrated with Rev_{34-50} peptide A. Relative binding affinities, K_{rel}, were determined as $K_a/K_{a,E1}$, where K_a is $1/K_d$. When the concentration of the RRE IIB model is much lower than K_d, K_d can be approximated as $([P] - r[P])/r$, where [P] is the molar concentration of total peptide and r is the fraction of ^{32}P-labeled RRE IIB model that has been bound by peptide (Weeks & Crothers, 1992). Bands labeled f represent free, labeled RRE model, and bands labeled b represent bound, labeled RRE model. Final RRE model concentrations were less than 1 nM. Full gel results for HP1, HP2, and the duplex titrated with Rev_{34-50} peptide A are available as Supporting Information.

Rev Peptide Characterization

The percent α-helicity of peptides was determined by circular dichroism as described in Chen et al. (1974), and the results (spectra not shown) are consistent with those described in Tan et al. (1993). Namely, Rev_{34-50} peptides with succinylated N termini and amidated C termini (peptides A and B) demonstrate a high degree of α-helical content, while the peptides with native termini (peptides C and D) demonstrate low α-helical content. The substitution Arg-39 → Lys found in peptides B and D had no significant effect on the α-helical content of the peptides.

Gel Shift Analysis of the RRE/Rev System

Relative Affinity of the RRE RNA Duplex for Rev_{34-50} Peptide A. Formation of complexes between Rev_{34-50} peptide A and the RRE RNA model hairpins, HP1 and HP2, as well as the RNA homoduplex (E1), was evaluated using gel shift analysis, and results are compared in Figure 5. HP1 and HP2 both bind Rev_{34-50} peptide A with an apparent binding affinity of 50−100 nM, which is consistent with previously reported results (Tan et al., 1993). The longer hairpin, HP1, appears to form unique complexes with additional Rev molecules upon increasing Rev peptide concentrations. The shorter hairpin, HP2, does not show evidence of additional Rev binding. Both HP1 and HP2 show general smearing on gels at higher Rev peptide concentrations, typical of nonspecific peptide binding. The RNA duplex, E1, requires higher Rev peptide concentrations to bring about formation of a nucleic acid/peptide complex and, correspondingly, a gel shift. Relative to the RNA duplex, E1, the binding affinities of HP1, HP2, and the RNA duplex are 10.0, 10.0, and 1.0, respectively, as described in Figure 5. In addition to a lower relative binding affinity, the RNA duplex shifts over a broader range of Rev peptide concentrations. It is important to note that all duplexes in these gel shift studies, including those composed of phosphodiester-linked oligonucleotides, migrated as intact duplexes under the gel shift

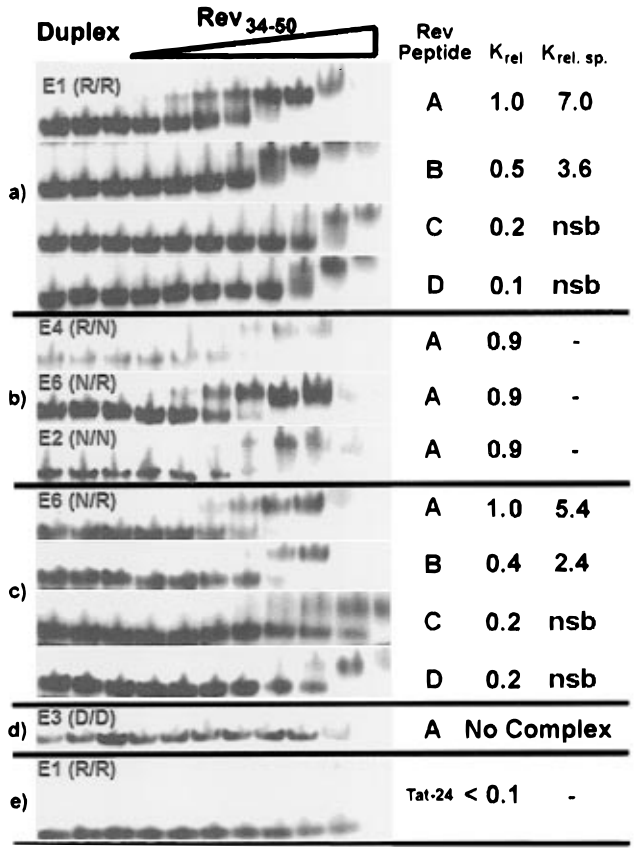

FIGURE 6: Gel shift assays of RRE IIB duplex models: (a) homoduplex E1 (R/R) titrated with Rev_{34-50} peptides A−D; (b) heteroduplexes E4 (R/N) and E6 (N/R) and homoduplex E2 (N/N) titrated with Rev_{34-50} peptide A; (c) heteroduplex E6 (N/R) titrated with Rev_{34-50} peptides A−D; (d) homoduplex E3 (D/D) representing the five phosphodiester-linked DNA-containing duplexes (E3, E5, E7, E8 and E9), all of which failed to form complexes with Rev_{34-50} peptide A; and (e) homoduplex E1 (R/R) titrated with the arginine-rich peptide, Tat-24. Relative binding affinities, K_{rel}, were determined as $K_a/K_{a,E1}$ as described in Figure 5. Full gel results for E1 and E6 titrated with Rev_{34-50} peptide A are available as Supporting Information. Complexes formed between duplexes E1 and E6 and Rev_{34-50} peptides C and D in parts a and c represent nearly nonspecific RNA/peptide interactions, and their K_{rel} values are approximate. Relative specificities, $K_{rel\ sp}$, were determined as K_{sp}/K_{nonsp}, which was defined as $K_a/K_{a,Rev_{34-50}peptide\ D}$ (Tan et al., 1993). The notation, nsb, means that the RRE/Rev complex cannot be discriminated from nonspecific interactions.

assay conditions described in Materials and Methods. In summary, the RRE duplex forms a specific complex with Rev peptide, as Pritchard et al. (1994) have shown for the RRE duplex/Rev protein interaction.

Relative Specificity of the RRE RNA Duplex for Rev_{34-50} Peptides A−D. The relative binding affinity of the RRE RNA duplex, E1 (R/R), for Rev_{34-50} peptide decreases with reduction of the α-helical content of the peptide. This is demonstrated by Rev_{34-50} peptides A versus C and B versus D in Figure 6a and is consistent with results reported by Tan et al. (1993) for the RRE hairpin (HP1). The data in Figure 6a also indicate that binding affinity decreases when Arg-39 is replaced by Lys (A versus B), again consistent with results reported by Tan et al. for the RRE hairpin (HP1). The relative binding affinity of peptides for the HP1 hairpin was assessed in the same way, and the results are parallel to those for the E1 duplex (data not shown). The specificity of the interactions between RNA duplex and the HP1 hairpin with Rev_{34-50} peptides confirms that the duplex/peptide complex is a good model system for comparative analysis. A more stringent assessment of the RRE duplex was performed where base substitutions G48 → A or G71 → A reduce formation of the complex with Rev_{34-50} peptide A, but cosubstitution enhances formation of complex (data not shown), which is consistent with Bartel et al. (1991) for the RRE hairpin (HP2) and Rev protein. Gait and co-workers (Pritchard et al., 1994) reached similar conclusions about the validity of duplex models for both RRE and TAR using Rev and Tat proteins, respectively. More recently, Wang et al. (1996) confirmed that a TAR duplex makes all contacts known to be required for high-affinity binding of Tat. The specificity of the duplex/peptide interaction under study is further underscored in Figure 6e, which demonstrates that the titration of RRE RNA duplex (E1) with arginine-rich Tat-24 peptide (Figure 2) produces the lowest K_{rel} value. The converse of this last experiment, TAR RNA duplex (T1) with Rev_{34-50} peptide A, also demonstrated a low relative binding affinity, as described later in this report.

Affinity and Specificity of the NP-DNA Duplex Model

NP-DNA-containing heteroduplexes (E4 and E6) as well as the NP-DNA homoduplex (E2) were compared for the ability to form complexes with Rev_{34-50} peptide A (Figure 6b). Clearly, N3′ → P5′ phosphoramidate DNA-containing duplexes bind Rev_{34-50} peptide A to the same degree that the RNA homoduplex, E1, binds this peptide as shown by similar K_{rel} values. Although the heteroduplex (E4) and the NP-DNA homoduplex (E2) visually appear to form smaller amounts of complex at the same peptide concentration, this is due to the underlabeling of these duplexes as described above. Analysis by microdensitometry clearly shows that the relative binding affinity of these duplexes is equivalent to that of the heteroduplex, E6. The heteroduplex, E6, was also complexed with Rev_{34-50} peptides A−D and analyzed by gel shift assay. The results presented in Figure 6c demonstrate that this heteroduplex (E6) matches both the relative binding affinity and the specificity of the RNA homoduplex (E1). This experiment shows that oligodeoxyribonucleotide N3′ → P5′ phosphoramidates form helices that are excellent RRE RNA mimetics from the standpoint of specific complex formation with Rev.

These observations are in dramatic contrast with results for RRE duplex models containing phosphodiester-linked DNA oligonucleotides (E3, E5, E7, E8 and E9), all of which failed to form complexes with Rev_{34-50} peptide A (Figure 6d; data for only the DNA homoduplex, E3, are shown). Clearly, N3′ → P5′ phosphoramidate DNA backbones differ dramatically from phosphodiester DNA backbones in their ability to present helical DNA structures that can be bound by Rev_{34-50} peptides.

Competitive Gel Shift Assays for RRE/Rev Interaction

To provide additional comparisons of relative binding affinities, competitive gel shift assays using unlabeled (cold) RRE RNA (E1) and NP-DNA-containing duplexes (E2, E4, and E6) and phosphodiester-linked DNA duplexes (E3) were performed. The competitive format was particularly attractive since it is unaffected by the underlabeling of the $N\text{-}E_b$ oligonucleotide. The results shown in Figure 7 demonstrate that the NP-DNA-containing duplexes compete with labeled RNA homoduplex (E1) for binding to Rev_{34-50} peptide A.

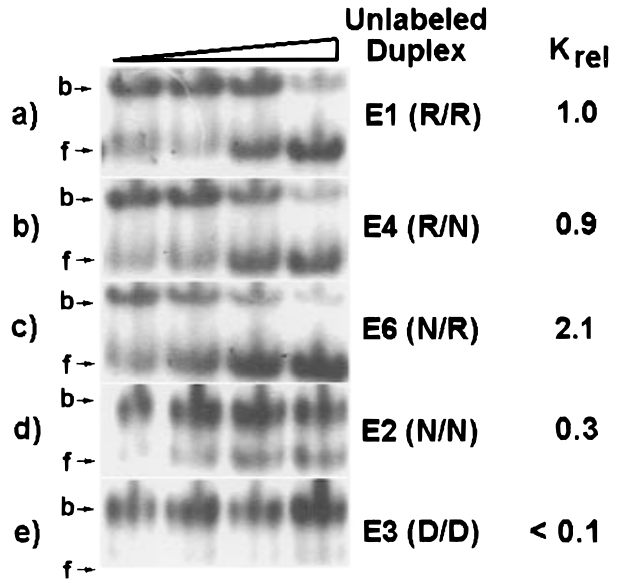

FIGURE 7: Competitive gel shift assays for inhibition of the formation of complex between RRE IIB RNA duplex (^{32}P-labeled duplex E1) and Rev_{34-50} peptide A. (a) Unlabeled homoduplex E1 (R/R) is the control inhibitor, which is compared with the unlabeled heteroduplexes (b) E4 (R/N) and (c) E6 (N/R), as well as with the unlabeled homoduplexes (d) E2 (N/N) and (e) E3 (D/D). K_{rel} is the reciprocal of the concentration of unlabeled competitor duplex required to reduce by 50% Rev_{34-50} peptide A binding to ^{32}P-labeled duplex E1 divided by the reciprocal concentration required of the unlabeled E1 (control), E2, E3, E4, and E6 duplex to achieve the same level of inhibition [variation of Pritchard et al. (1994)]. This rendering means that strong competitive inhibitors have K_{rel} values greater than 1.0. Bands labeled f and b refer to free and bound labeled duplex as in Figure 5.

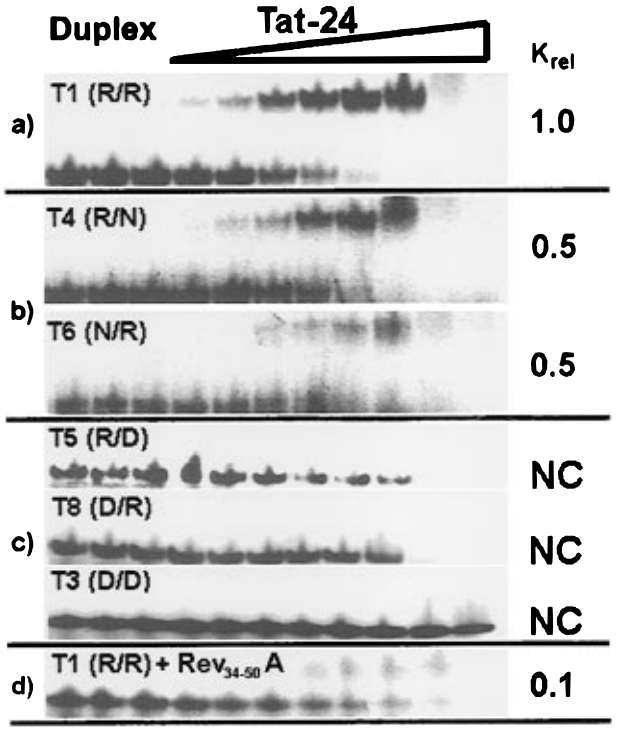

FIGURE 8: Gel shift assays of TAR duplex models: (a) homoduplex T1 (R/R) titrated with Tat-24 peptide, (b) titration of N3′ → P5′ phosphoramidate-containing heteroduplexes T4 (R/N) and T6 (N/R) [data for the homoduplex T2 (N/N) are not shown], (c) titration of O3′ → P5′ phosphodiester-containing heteroduplexes T5 (R/D) and T8 (D/R) and the homoduplex T3 (D/D), and (d) titration of the homoduplex T1 (R/R) with the arginine-rich peptide, Rev_{34-50} peptide A. Relative binding affinities were determined as $K_a/K_{a,T1}$ as described in Figure 5 for the binding of RRE to Rev. NC means that no complex was isolated.

The order of inhibition as determined by microdensitometry is E6 > E1 > E4 > E2. The phosphodiester-linked DNA homoduplex (E3) failed to inhibit RRE/Rev interaction at duplex concentrations as high as 20 μM.

Gel Shift Analysis of the TAR/Tat System

Affinity and Specificity of the TAR RNA and NP-DNA Duplex Models. The TAR/Tat interaction (Figure 2) provided a second, distinct opportunity to test the ability of N3′ → P5′ phosphoramidate DNAs to mimic RNA structures. The TAR RNA homoduplex (T1), heteroduplexes (T4 and T6), and NP-DNA homoduplex (T2) were each titrated with Tat-24 peptide under the same experimental conditions used for RRE/Rev. The gel shift analysis in Figure 8 shows that the relative binding affinity of the RNA homoduplex (T1) is the greatest, followed by that of both T4 (R/N) and T6 (N/R). The homoduplex, T2, on the other hand, did not produce sufficient signal due to underlabeling, and no gel result is presented. However, analysis by microdensitometry did show that the T2 duplex shifts at approximately the same peptide concentration as T4 and T6. Consistent with the RRE data, Figure 8 shows that TAR duplex models containing phosphodiester DNA oligonucleotides (T3, T5, and T8) failed to form complexes with Tat-24 peptide that are detectable by gel electrophoresis. The TAR RNA homoduplex (T1) demonstrated a low relative binding affinity for the arginine-rich Rev_{34-50} peptide A, which underscores the specificity of the TAR/Tat interaction. The results in Figure 8 confirm the fact that NP-DNA oligonucleotides form A-type helices that can bind specifically to RNA-binding peptides. Figure 9 demonstrates that the NP-DNA-containing duplexes compete with labeled RNA homoduplex (T1) for binding to Tat-24. The phosphodiester-linked DNA homoduplex (T3) failed to inhibit TAR/Tat interaction at duplex concentrations as high as 20 μM.

DISCUSSION

Biophysical studies of complementary N3′ → P5′ phosphoramidates (NP-DNAs) indicated that these DNA analogs form an A-type duplex structure, in spite of their deoxyribose sugars, and strongly suggested the possibility that NP-DNAs could mimic structural RNAs and bind specifically to RNA-binding proteins. A structural RNA mimetic consisting of NP-DNAs would be nuclease-resistant and have the potential for competitively inhibiting the formation of important RNA/protein complexes such as RRE/Rev and TAR/Tat in HIV-1 infected cells. On the other hand, numerous studies have shown that the 2′-hydroxyl group is a key feature to the structure, hydration, and stability of RNA molecules (Egli et al., 1996; Portmann et al., 1995), and it was not clear whether the 2′-OH group could be completely deleted to yield an RNA mimetic that would bind strongly to RNA-binding proteins like Rev and Tat. It has been shown, for example, that replacement of only a few key nucleotides in RRE or TAR by deoxyribose sugars with a phosphodiester linkage significantly decreases Rev and Tat binding (Pritchard et al., 1994).

The results presented in this paper, however, demonstrate that NP-DNAs are excellent RNA mimetics and have potential as competitive inhibitors of viral function. RRE and TAR duplex models containing N3′ → N5′ phosphora-

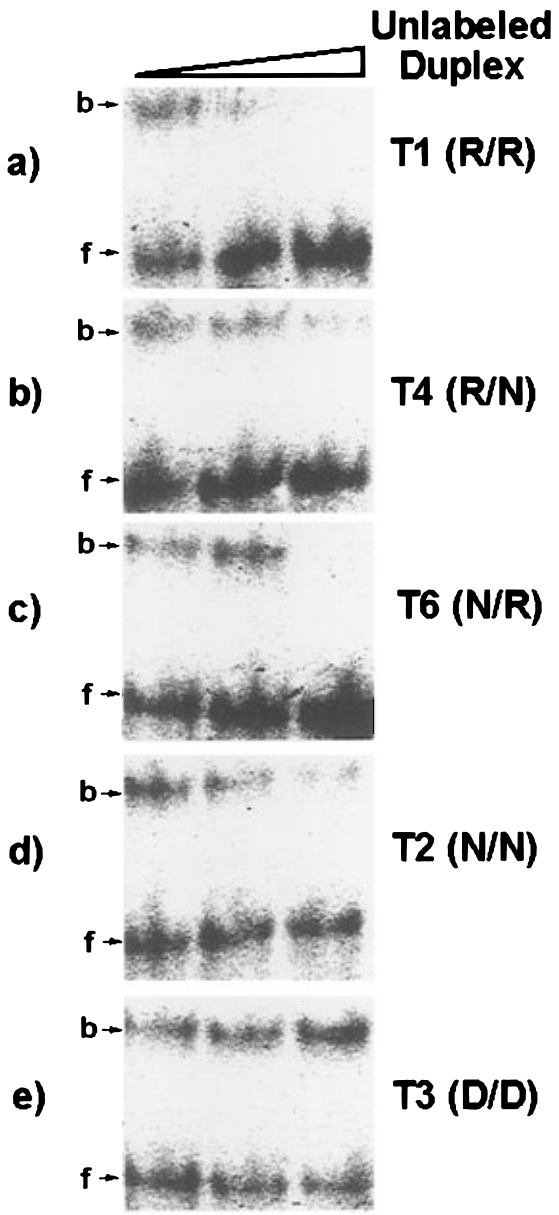

FIGURE 9: Competitive gel shift assays for inhibition of the formation of the complex between TAR RNA duplex (^{32}P-labeled duplex T1) and Tat-24. (a) Unlabeled homoduplex T1 (R/R) is the control inhibitor, which is compared with the unlabeled heteroduplexes (b) T4 (R/N) and (c) T6 (N/R), as well as with the unlabeled homoduplexes (d) T2 (N/N) and (e) T3 (D/D).

midate backbones are clearly A-form helices in solution that form complexes with respective Rev and Tat-related peptides with the same high affinity and specificity demonstrated by RRE and TAR RNAs. As structural RNA mimetics, NP-DNA-containing duplexes also competitively inhibit the formation of RRE/Rev and TAR/Tat complexes to the same degree that isosequential RNAs inhibit these complexes. These observations and the promising studies of endogenous RNA decoys (Bevec et al., 1994; Gilboa & Smith, 1994; Lee et al., 1995; Malim et al., 1992) suggest that there are new, exciting possibilities for exogenous RNA mimetics consisting of oligodeoxyribonucleotide N3′ → N5′ phosphoramidates.

Fully complementary NP-DNA helices adopt an A-form structure, making them quite similar to isosequential RNA duplexes and decidedly different than isosequential DNAs as judged by CD and high-field NMR (Gryaznov et al., 1995; Ding et al., 1996). This observation along with their enhanced duplex stability is quite surprising, since the NP-DNA sugars lack the 2′-hydroxyl group that has been suggested to be responsible for many of the unique properties of RNA (Egli et al., 1996; Portmann et al., 1995). In our study of the perturbed duplex found in RRE IIB, duplex models containing NP-DNA oligonucleotides have T_ms that are markedly higher than those of duplex models containing DNA strands. Moreover, RRE NP-DNA duplexes are clearly A-form helices, which is consistent with previously published reports (Gryaznov et al., 1995; Ding et al., 1996). The 2′-OH group is not required for formation of A-type helices even in highly perturbed duplexes. The replacement of the 3′-oxygen with the NH group removes the normally predominant gauche effect and allows the anomeric effect to dominate, thus driving the pentofuranose moiety into the N-pseudorotamer (Thibaudeau et al., 1994). Therefore, NP-DNA homoduplexes adopt an A-form helical structure without any requirement for a steric, hydration (Egli et al., 1996; Portmann et al., 1995), or other effect from 2′-hydroxyl groups, which are missing in NP-DNAs.

Our data show that RRE and TAR NP-DNA-containing duplexes (E2, E4, and E6 and T2, T4, and T6) bind to and compete for respective Rev and Tat peptides (Figures 6−9), and these data are consistent with NMR-based reports which demonstrate that 2′-OH groups are apparently not required for binding with high affinity or specificity (Battiste et al., 1995, 1996; Puglisi et al., 1992; Ye et al., 1995). This may be somewhat expected for the TAR/Tat interaction because substitutions of several ribonucleotides with deoxyribonucleotides in TAR did not demonstrate a significant change in affinity for Tat (Hamy et al., 1993; Pritchard et al., 1994; Sumner-Smith et al., 1991). However, the RRE/Rev interaction has been shown to be substantially altered by replacement of ribonucleotides in the internal loop with deoxyribonucleotides (Iwai et al., 1992; Pritchard et al., 1994). Our data suggest that this reduction in binding is not due to the loss of 2′-OH groups but rather to the replacement of one sugar conformation with another. RRE and TAR duplexes containing phosphodiester-linked DNA oligonucleotides (E3, E5, E7, E8, and E9 and T3, T5, and T8) have deoxyribose sugars as with the N3′ → P5′ phosphoramidate DNA oligonucleotides; however, phosphodiester-linked DNA duplexes possess too much B-form character (Figure 4a,b) to bind Rev and Tat or competitively inhibit RRE/Rev or TAR/Tat interaction, respectively (Figures 6−9).

All N3′ → P5′ phosphoramidate-linked DNA and phosphodiester-linked DNA oligonucleotides used in Rev and Tat binding studies contained d(U) bases instead of d(T) bases. This substitution removes C5-methyl groups from the major groove of the resulting helices. Since Rev and Tat are known to bind in the respective major grooves of RRE (Battiste et al., 1995) and TAR (Puglisi et al., 1992; Wang et al., 1996), we wanted to assure that NP-DNAs would not be inadvertantly compromised as peptide receptors from the start. The presence of d(U) bases in the RRE DNA duplex, E3, had no apparent effect on helical conformation. The CD spectrum for E3 with d(U) bases was virtually superimposable on the CD spectrum for E3 with d(T) bases (spectra not shown).

The RRE RNA homoduplex, E1 (R/R), displays an elevated T_m (54.2 °C) relative to isosequential DNA [E3 (D/D)], which dissociates at 44.2 °C (Table 3). E1 is A-form

by CD, whereas E3 is in the B-form helical family (Figure 4a). E1 binds Rev_{34-50} peptides with a relative affinity and specificity that is comparable to those of extensively studied hairpin/peptide interactions (Figure 5; gel shift data for HP1 and HP2 with Rev_{34-50} peptides B−D are not shown) (Tan et al., 1993). In sharp contrast, E3 does not significantly bind Rev_{34-50} peptide under the same conditions (Figure 6d), nor does E3 competitively inhibit RRE/Rev interaction (Figure 7e). When one substitutes an NP-DNA oligonucleotide into E1, the resulting heteroduplex, E6 (N/R), has a T_m of 60.8 °C with a sharp, cooperative transition that is elevated with respect to both E1 and E8 (D/R; 41.5 °C) and is consistent with our previous reports on NP-DNA duplexes (Gryaznov et al., 1995; Ding et al., 1996). The E6 duplex is the most A-form heteroduplex by CD (Figure 4b), and its spectrum is nearly superimposable on the spectrum of the RNA homoduplex, E1, in the 220−270 nm region. E6 displays a relative affinity and specificity for Rev_{34-50} peptides A−D (Figure 6b,c) that parallel those of the RNA homoduplex, E1 (Figure 6a), as well as those of the HP1 and HP2 hairpins (Figure 5). Clearly, the NP-DNA oligonucleotide in the E6 heteroduplex (N-E_a) is mimicking the RNA oligonucleotide it has supplanted (R-E_a). Competitive gel shift assays confirm this mimicry in Figure 7c, where E6 competes reproducibly to a greater extent than the control RNA homoduplex, E1, for Rev_{34-50} peptide A. In striking contrast, the DNA homoduplex, E3 (D/D) in Figure 7e, failed to inhibit RRE/Rev interaction at duplex concentrations as high as 20 μM.

The converse of the E6 heteroduplex, E4 (R/N), has a T_m of 54 °C, which is lower than the T_m for E6 but equals the T_m of the RNA homoduplex, E1. The T_ms for E4 and E1 are both considerably higher than those for the DNA-containing duplexes, E3 (D/D; 44.2 °C) and E5 (R/D; 45.0 °C), which is again consistent with earlier reports on NP-DNA duplexes. The thermal dissociation curve of E4 is unusually broad; however, the individual oligonucleotides in E4, R-E_a, and N-E_b, can form fully complemented duplexes with DNA (C1 and C4, respectively) that dissociate in a cooperative fashion (Figure 3 and Table 3). It is also important to note that the C4 duplex (fcD/N) dissociated at 68.3 °C, whereas C6 (fcD/D) dissociated at a lower temperature of 60.2 °C, suggesting that the N-E_b oligonucleotide forms a duplex that behaves in a manner similar to that of canonical, base-paired structures. Gel shift analysis of the E4 heteroduplex titrated with Rev_{34-50} peptide A (Figure 6b) shows that E4 has a relative binding affinity that is comparable to that of both the RNA homoduplex, E1, and the E6 heteroduplex and the NP-DNA homoduplex, E2. However, as Figure 7b shows, the E4 duplex persistently demonstrated a lower level of competitive inhibition than both the E1 (control) and E6 duplexes.

The NP-DNA homoduplex, E2, has an elevated T_m of 58 °C and an A-form CD spectrum, characteristics held in common by the strong competitive inhibitors, E1 (control; 54.2 °C) and E6 (60.8 °C) duplexes. The T_m for E2 of 58 °C is greater than the T_m for E4 (54 °C), but the melting curves for both duplexes are characterized by broad transitions. E2 binds Rev_{34-50} peptide A with an affinity comparable to that of the RNA homoduplex, E1 (Figure 6b), and clearly, E2 acts as an RNA decoy. However, competitive gel shift analysis (Figure 7) shows E2 as a significantly poorer competitive inhibitor where the rank order is E6 > E1 > E4 > E2 >> E3. The differences in K_{rel} that exist between the gel shift titrations (Figure 6) and competitive gel shift assays (Figure 7) point to the possible advantages of the latter format, which can detect subtle interaction differences between nucleic acids and peptides (Weeks & Crothers, 1992).

NMR analyses of the RRE RNA/Rev peptide complex (Battiste et al., 1995, 1996) show that RRE IIB could be difficult to mimic due to a perturbation in the phosphodiester backbone at G71-U72, which lies along the RRE E_b sequence (Figure 1b). The backbone reverses its polarity in this region to allow G71 to form a G71·G48 base pair with both glycosidic torsions *anti* and U72 unstacked. In the RRE duplex model (Figure 1b), the N-E_b oligonucleotide contains G71 and U72, and duplexes containing this oligonucleotide [E2 (N/N) and E4 (R/N)] exhibit reduced inhibition of RRE/Rev interaction (Figure 7b,d), possibly due to increased rigidity of the phosphoramidate backbone (Ding et al., 1996).

The E2 duplex presents additional characteristics that might provide another reason for its reduced capacity as a competitive inhibitor. The CD spectrum of E2 is clearly deviating from the CD spectra of both the A-form E1 and E6 duplexes at the 210 and 290 nm negative and 265 nm positive bands, as well as in the 220 to 270 nm region (Figure 4a,b). The E2 spectrum is most similar to the E4 spectrum, and CD results for the E1 and E2 duplexes are consistent with analogous spectra in Gryaznov et al. (1995) and Ding et al. (1996). These data suggest that the NP-DNA homoduplex, E2, is assuming an A-form structure that, although similar to the RNA homoduplex, is distinct from the RNA homoduplex. This is consistent with recent NMR and modeling studies in our laboratory, which show that NP-DNA homoduplexes are most accurately represented by the A′-DNA structure within the A-form helical family (unpublished results).

It is strikingly clear from Figures 6a−c and 7a−d that the RRE RNA duplex E1 is mimicked by NP-DNA duplexes E2, E4, and E6. Phosphodiester-linked DNA-containing duplexes, on the other hand, are completely discriminated against by Rev_{34-50} peptide A, as represented in Figures 6d and 7e. We conclude that the RNA major groove-binding Rev_{34-50} peptide A binds with high affinity and specificity to RRE homo- and heteroduplexes comprised of RNA and NP-DNA oligonucleotides and that this peptide probe is incapable of recognizing the B-form major groove of isosequential phosphodiester-linked DNA duplexes. The specificity of this recognition is underscored by Figure 6e, which shows that the RNA duplex, E1, fails to bind the arginine-rich peptide, Tat-24, with high affinity. The differences between N3′ → P5′ phosphoramidate-linked oligonucleotides and phosphodiester-linked oligonucleotides of the same sequence are dramatic and clear.

The data also demonstrate that oligodeoxyribonucleotide N3′ → P5′ phosphoramidates can serve as structural RNA mimetics in an RNA/peptide system that is distinct from the RRE/Rev system. The TAR RNA homoduplex, T1, forms a complex with Tat-24 that is stable to partition on polyacrylamide gels (Figure 8a). Substituting NP-DNA oligonucleotides into the T1 duplex to form heteroduplexes T4 and T6 has only a modest effect on the relative binding affinity of the TAR/Tat interaction. The poor end labeling of both TAR NP-DNA oligonucleotides under study made the preparation an autoradiograph for the homoduplex T2

problematic; however, low-level signals from the T2 duplex did shift at roughly the same peptide concentration as for T4 and T6. Consistent with the results from the study of RRE/Rev interaction, the TAR DNA homoduplex (T3), as well as the DNA/RNA heteroduplexes, T5 and T8, all failed to form complexes with Tat-24 that were stable to partition on polyacrylamide gels.

Inefficient end labeling of the TAR NP-DNA oligonucleotides made the competitive gel shift format particularly attractive. Competitive gel shift assays for inhibition of the formation of TAR/Tat complexes (Figure 9) are consistent with RRE/Rev results in that unlabeled heteroduplexes T4 (R/N) and T6 (N/R) inhibited TAR/Tat to a degree that is comparable to that of the control inhibitor, the RNA homoduplex T1. The DNA homoduplex, T3, failed to inhibit TAR/Tat interaction.

In summary, our study of two distinct RNA/peptide interactions in HIV-1 has clearly demonstrated that N3′ → P5′ phosphoramidate DNA analogs of the structural RNAs, RRE and TAR, can effectively function as structural RNA mimetics. We have shown that RNAs now have a valid surrogate, a nuclease-resistant analog that adds a new dimension to the search for effective therapeutic agents against viral diseases. The goal of an effective therapeutic against a lethal disease clearly represents the most challenging potential application of NP-DNA oligonucleotides. However, the potential advantages of NP-DNA oligonucleotides as nuclease-resistant RNA surrogates in RNA research and as potential diagnostic reagents are also promising, making further research on oligonucleotide N3′ → P5′ phosphoramidates of great interest.

SUPPORTING INFORMATION AVAILABLE

Full gel shift assays of the RRE IIB hairpins HP1 and HP2, as well as of the homoduplex E1 (R/R) and heteroduplex E6 (N/R), titrated with Rev_{34-50} peptide A as shown in Figures 5 and 6a,c (2 pages). Ordering information is given on any current masthead page.

REFERENCES

Bartel, D. P., Zapp, M. L., Green, M. R., & Szostak, J. W. (1991) *Cell 67*, 529−536.

Battiste, J. L., Tan, R., Frankel, A. D., & Williamson, J. R. (1995) *J. Biomol. NMR 6*, 375−389.

Battiste, J. L., Mao, H., Rao, N. S., Tan, R., Muhandiram, D. R., Kay, L. E., Frankel, A. D., & Williamson, J. R. (1996) *Science 273*, 1547−1551.

Bevec, D., Volcplatzer, B., Zimmermann, K., Dobrovnik, M., Hauber, J., Veres, G., & Bohnlein, E. (1994) *Hum. Gene Ther. 5*, 193−201.

Chang, H. K., Lisziewicz, J., Gallo, R. C., & Ensoli, B. (1993) *J. Acquired Immune Defic. Syndr. 6*, 706 (abstract).

Chen, J.-K., Schultz, R. G., Lloyd, D. H., & Gryaznov, S. M. (1995) *Nucleic Acids Res. 23*, 2661−2668.

Chen, Y.-H., Yang, J. T., & Chau, K. H. (1974) *Biochemistry 13*, 3350−3359.

Clusel, C., Meguenni, S., Elias, I., Vasseur, M., & Blumenfeld, M. (1995) *Gene Expression 4*, 301−309.

Cook, K. S., Fisk, G. J., Hauber, J., Usman, N., Daly, T. J., & Rusche, J. R. (1991) *Nucleic Acids Res. 19*, 1577−1582.

Creighton, T. E. (1993) in *Proteins: Structure and Molecular Properties*, W. H. Freeman and Co., New York.

Cullen, B. R., & Malim, M. H. (1991) *Trends Biochem. Sci. 16*, 346−350.

Daly, T. J., Doten, R. C., Rennert, P., Auer, M., Jaksche, H., Donner, A., Fisk, G., & Rusche, J. R. (1993) *Biochemistry 32*, 10497−10505.

DeDionisio, L., & Gryaznov, S. M. (1995) *J. Chromatogr. 669*, 125−131.

Ding, D., Gryaznov, S. M., Lloyd, D. H., Chandrasekaran, S., Yao, S., Ratmeyer, L., Pan, Y., & Wilson, W. D. (1996) *Nucleic Acids Res. 24*, 354−360.

Egli, M., Portmann, S., & Usman, N. (1996) *Biochemistry 35*, 8489−8494.

Gilboa, E., & Smith, C. (1994) *Trends Genet. 10*, 139−144.

Gryaznov, S. M., Lloyd, D. H., Chen, J. K., Schultz, R. G., DeDionisio, L. A., Ratmeyer, L., & Wilson, W. D. (1995) *Proc. Natl. Acad. Sci. U.S.A. 92*, 5798−5802.

Hamy, F., Assleine, U., Grasby, J., Iwai, S., Pritchard, C., Slim, G., Butler, P. J., Karn, J., & Gait, M. J. (1993) *J. Mol. Biol. 230*, 111.

Iwai, S., Pritchard, C., Mann, D. A., Karn, J., & Gait, M. J. (1992) *Nucleic Acids Res. 20*, 6465.

Kibler-Herzog, L., Kell, B., Zon, G., Shinozuka, K., Mizan, S., & Wilson, W. D. (1990) *Nucleic Acids Res. 18*, 3545−3555.

Kjems, J., Brown, M., Chang, D. D., & Sharp, P. A. (1991) *Proc. Natl. Acad. Sci. U.S.A. 88*, 683−687.

Lee, S. W., Gallardo, H. F., Gaspar, O., Smith, C., & Gilboa, E. (1995) *Gene Ther. 2*, 377−384.

Long, K. S., & Crothers, D. M. (1995) *Biochemistry 34*, 8885−8895.

Malim, M. H., Hauber, J., Le, S.-Y., Maizel, J. V., & Cullen, B. R. (1989) *Nature 338*, 254−257.

Malim, M. H., Freimuth, W. W., Liu, J. S., Boyle, T. J., Lyerly, H. K., Cullen, B. R., & Nabel, G. J. (1992) *J. Exp. Med. 176*, 1197−1201.

Mann, D. A., Mikaelian, I., Zemmel, R. W., Green, S. M., Lowe, A. D., Kimura, T., Singh, M., Butler, P. J. G., Gait, M. J., & Karn, J. (1994) *J. Mol. Biol. 421*, 193−207.

Milligan, J. F., & Uhlenbeck, O. C. (1989) *Methods Enzymol. 180*, 51−62.

Mountzouris, J. A., & Hurley, L. H. (1996) in *Bioorganic Chemistry: Nucleic Acids* (Hecht, S. M., Ed.) pp 288−323, Oxford University Press, New York.

Nelson, J. S., Giver, L., Ellington, A. D., & Letsinger, R. L. (1996) *Biochemistry 35*, 5339−5344.

Portmann, S., Usman, N., & Egli, M. (1995) *Biochemistry 34*, 7569−7575.

Pritchard, C. E., Grasby, J. A., Hamy, F., Zacharek, A. M., Singh, M., Karn, J., & Gait, M. J. (1994) *Nucleic Acids Res. 22*, 2592−2600.

Puglisi, J. D., Tan, R., Calnan, B. J., Frankel, A. D., & Williamson, J. R. (1992) *Science 257*, 76−80.

Ratmeyer, L., Zapp, M., Green, M., Vinayak, R., Kumar, A., Boykin, D. W., & Wilson, W. D. (1996) *Biochemistry 35*, 13689−13696.

Rosen, C. A., Sodroski, J. G., & Haseltine, W. A. (1985) *Cell 41*, 813.

Sambrook, J., Fritsch, E. F., & Maniatis, T. (1989) in *Molecular Cloning: A Laboratory Manual* (Nolan, C., Ed.) pp 6.36−6.48, Cold Spring Harbor Laboratory Press, Plainview, NY.

Sumner-Smith, M., Roy, S., Barnett, R., Reid, L. S., Kuperman, R., Delling, U., & Sonenberg, N. (1991) *J. Virol. 65*, 5196.

Sundquist, W. I. (1996) *Nat. Struct. Biol. 3*, 8−11.

Symensma, T. L., Giver, L., Zapp, M., Tackle, G. B., & Ellington, A. D. (1996) *J. Virol. 70*, 179−187.

Tan, R., Chen, L., Buettner, D. H., & Frankel, A. D. (1993) *Cell 73*, 1031−1040.

Thibaudeau, J. P., Garg, N., Papchikhin, A., & Chattopadhyaya, J. (1994*) J. Am. Chem. Soc. 116*, 4038−4043.

Tiley, L. S., Malim, M. H., Tewary, H. K., Stockley, P. G., & Cullen, B. R. (1992) *Proc. Natl. Acad. Sci. U.S.A. 89*, 758−762.

Wang, Z., & Rana, T. M. (1996) *Biochemistry 35*, 6491−6499.

Weeks, K. M., & Crothers, D. M. (1992) *Biochemistry 31*, 10281−10287.

Weiss, R. B. (1992) *Semin. Oncol. 19*, 670−686.

Wilson, W. D., Tanious, F. A., Fernandez-Saiz, M., & Rigl, C. T. (1996) *Methods Mol. Med.* (in press).

Ye, X., Kumar, R. A., & Patel, D. J. (1995) *Chem. Biol. 2*, 827−840.

Zapp, M. L., Stern, S., & Green, M. R. (1993) *Cell 74*, 969−978.

BI961980W